Steel and Composite Structures, *Vol. 23, No. 4 (2017) 473-481*
DOI: https://doi.org/10.12989/scs.2017.23.4.473

Flexural behavior of beams in steel plate shear walls

Ying Qin*, Jin-Yu Lu, Li-Cheng-Xi Huang and Shi Cao

Key Laboratory of Concrete and Prestressed Concrete Structures of the Ministry of Education, Southeast University, Nanjing, China

(*Received July 09, 2016, Revised January 04, 2017, Accepted January 20, 2017*)

Abstract. Steel plate shear wall (SPSW) system has been increasingly used for lateral loads resisting system since 1980s when the utilization of post-buckling strength of SPSW was realized. The structural response of SPSWs largely depends on the behavior of the surrounded beams. The beams are normally required to behave in the elastic region when the SPSW fully buckled and formed the tension field action. However, most modern design codes do not specify how this requirement can be achieved. This paper presents theoretical investigation and design procedures of manually calculating the plastic flexural capacity of the beams of SPSWs and can be considered as an extension to the previous work by Qu and Bruneau (2011). The reduction in the plastic flexural capacity of beam was considered to account for the presence of shear stress that was altered towards flanges at the boundary region, which can be explained by Saint-Venant's principle. The reduction in beam web was introduced and modified based on the research by Qu and Bruneau (2011), while the shear stress in the web in this research is excluded due to the boundary effect. The plastic flexural capacity of the beams is given by the superposition of the contributions from the flanges and the web. The developed equations are capable of predicting the plastic moment of the beams subjected to combined shear force, axial force, bending moment, and tension fields induced by yielded infill panels. Good agreement was found between the theoretical results and the data from previous research for flexural capacity of beams.

Keywords: steel plate shear wall; beam; flexural behavior; Saint-Venant's principle; capacity

1. Introduction

Steel plate shear wall (SPSW) system has been increasingly used in North America and Asia as the lateral load resisting system in recent years (Chatterjee *et al*. 2015). A SPSW is composed of a steel structural frame infilled with web plates, as shown in Fig. 1. SPSWs offer excellent structural and architectural merits over traditional reinforced concrete shear walls, especially in terms of acceptable wall thickness, reduced entire weight, and aesthetic appearance. Furthermore, the applications of SPSW facilitate construction and increases usable floor area.

A number of researches have been undertaken on the structural performance of SPSWs. Previous studies on the experimental behavior of SPSW have included that of Lubell *et al*. (2000), Guo *et al*. (2011), Clayton *et al*. (2013), Guo and Yuan (2015), He *et al*. (2015), and Sabouri-Ghomi and Mamazizi (2015). Lubell *et al*. (2000) tested two single- and one four-story SPSWs under repeated loadings. The results indicated that SPSWs exhibited good energy dissipation capacity and ductility. Guo *et al*. (2011) experimentally studied the SPSWs connected to boundary beams only to prevent the premature failure of boundary columns. Clayton *et al*. (2013) proposed the self-centering SPSWs and the results of a series of quasi-static cyclic tests indicated that the specimens were capable of resisting lateral loads while reducing the structural repair costs and loss of building functionality. Guo and Yuan (2015) conducted cyclic testing on six novel SPSW specimens trilaterally constrained with an elastic restraint side. He *et al*. (2015) tested SPSWs with double-tapered links and in-plane reference. Sabouri-Ghomi and Mamazizi (2015) studied experimentally the effects of openings on the structural behavior of SPSWs.

Previous studies on the analytical response of SPSW have been conducted by Berman and Bruneau (2003), Sahoo *et al*. (2015), Vatansever and Berman (2015), Zirakian and Zhang (2015), Dhar and Bhowmick (2016), Bahrebar *et al*. (2016), and Rahmzadeh *et al*. (2016). Berman and Bruneau (2003) proposed a procedure for design of SPSWs using plastic analysis of the strip model. Sahoo *et al*. (2015) used finite element analysis to assessed the impact of different typed of HBE-to-VBE connections on the overall behavior of SPSW under cyclic loadings. Vatansever and Berman (2015) developed a behavior model for screw connections to represent the nonlinear response of thin SPSWs. Zirakian and Zhang (2015) evaluated the structural performance of SPSWs with unstiffened low yield point steel web panels according to AISC 341. Dhar and Bhowmick (2016) investigated the seismic demands of ductile unstiffened SPSWs by multi-mode pushover analysis and modal pushover analysis methods. Bahrebar *et al*. (2016) investigated the buckling stability, strength, stiffness, and ductility of SPSWs using finite element models. Rahmzadeh *et al*. (2016) applied finite element analysis to assess the impact of rigidity and arrangement of stiffeners on the buckling response of SPSWs.

On the other hand, there is a dearth of information on

*Corresponding author, Assistant Professor,
E-mail: qinying@seu.edu.cn

ISSN: 1229-9367 (Print), 1598-6233 (Online)

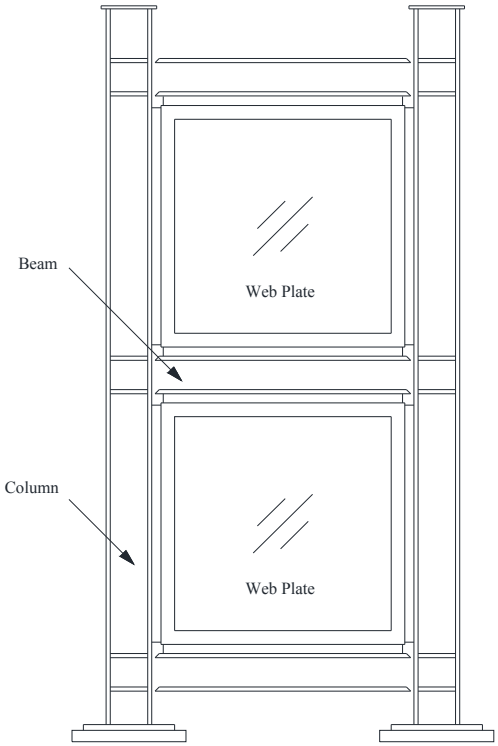

Fig. 1 Configuration of SPSW

the structural behavior of boundary element members (i.e., boundary beams and columns). Some preliminary research on design of boundary columns has included that of Park *et al*. (2007), and Berman and Bruneau (2008). Park *et al*. (2007) presented a simplified approach for predicting the axial and flexural demands on the columns. Berman and Bruneau (2008) used free body diagrams to determine the ultimate moment, axial and shear force demands for columns in SPSWs. For the research on boundary beams in SPSWs, Qu and Bruneau (2010) proposed an analytical model, which combined the assumed plastic mechanism with a linear beam model of intermediate beams considering fully yielded web plates, for approximating the capacity demands of intermediate beam with reduced beam section. In their study, the analytical procedure proposed by Qu and Bruneau (2011), which considered the reduced axial yield strength due to the presence of vertical component of tension field on the beams, was adopted to predict the plastic flexural capacity of the beams. However, the boundary effects, as will be described later in this paper, were not considered to account for the possible reduction in flexural capacity of the flanges, which overestimates the plastic moment of the beam and leads to the design on the unconservative side. Recently, Moghimi and Driver (2014) presented an analysis method, which was based on the principle of capacity design and nonlinear finite element simulations, for evaluating the axial force demands in the beam.

The Chinese technical specification for steel plate shear walls JGJ/T380-2015 (2015) offers the shear capacity of SPSWs for walls connected to either boundary frame or boundary beams only. Meanwhile, the requirement for the moment of inertia of boundary column is specified. However, there is a lack of information on the requirement for the boundary beam.

Meanwhile, the widely-acknowledged opinion, which considers that the fully restrained beam-to-column connection in steel moment resisting frames can be designed based on the assumption that the classical beam theory holds, is largely challenged during the 1994 Northridge and 1995 Kobe earthquakes. Fully-restrained steel moment frames were once regarded as being among the most ductile systems and essentially invulnerable to earthquake-induced structural damage. However, a number of steel moment resisting frames were found to have experienced obvious damages at the connections during these two earthquakes. The observation of damages can be attributed to a number of different factors, among which one of the most important issues is the boundary effects as mentioned by Lee (2006). Due to the restraint of column face to the beam cross section, the stress distribution in the beam near the connection does not follow the Euler-Bernoulli hypothesis of plane sections. The shear stress, which is assumed to be carried largely by the beam web, tends towards beam flanges. This causes the flanges suffering from overloading while leaves large parts of the beam web devoid of shear stress. Therefore, it is necessary to develop analytical procedures to account for this effect, to correctly predict the flexural capacity, and in addition to guarantee the elastic response of beams.

The work presented in this paper attempts to address this issue by developing a simple manual calculation procedure for the flexural capacity of beam in SPSWs subjected to combined forces based on traditional plastic theory and free body diagrams. In this research, the yield mechanism of SPSWs was introduced according to the research by Berman and Bruneau (2003), and the boundary effect on the force transfer mechanism was comprehensively discussed, which is the main originality of this research. The axial yield strength of the flanges were reduced to account for the presence of shear stress due to the restraint of column face. Furthermore, the influence of vertical component of tension field on beams induced by web plates was introduced. The method and idea was based on the research by Qu and Bruneau (2011), while the shear stress in the web was absent in this research due to the boundary effect. The calculated flexural capacity of beams was then obtained from the summation of the contributions from the web and flanges. Validity of the proposed methodology was demonstrated through comparisons against previous research results. The work in this paper provides basis for further development of capacity design model of beams of SPSWs.

2. Expected yielding mechanism of SPSW

For multistory SPSWs with rigid beam-to-column connections subjected to lateral loads, two main plastic mechanisms were identified by Berman and Bruneau (2003) that should be considered in predicting the flexural behavior of beams, i.e., soft-story plastic mechanism and uniform yielding mechanism. In soft-story plastic mechanism, the plastic hinges would form in columns at a single story. Most

of the earthquake energy is absorbed by the stories above the soft-story. In contrast, the possible collapse mechanism of multistory SPSWs involving uniform yielding of web plates over each story is more preferable, since in this case the earthquake energy is distributed over entire structure height.

It has been pointed out by Berman and Bruneau (2003) that the actual yielding mechanism is normally somewhere between a soft-story mechanism and uniform yielding mechanism. However, for the purpose of evaluating the flexural capacity of beams in SPSW in this paper, there is no need to exactly figure out the most adequate yielding mechanism. It is always conservative to use the uniform yielding mechanism as the web plates undergo larger inelastic deformation in this case, which eventually results in greater force demands in the beam. Therefore, the uniform yielding mechanism will be selected in this research for prediction of plastic flexural capacity of beams in SPSWs.

The web plates form the inclined tension field action when the SPSW develops the desired yielding mechanism. The tension field on the beam can be decomposed into the vertical (ω_{ybi}) and horizontal components (ω_{xbi}), respectively, as can be calculated based on Eqs. (1)-(2) (Berman and Bruneau 2008). Furthermore, axial compressive force (P) is generated in the beam due to the boundary moment frame sway, horizontal components of tension field on columns, and vertical and horizontal components of tension fields on beams (Qu and Bruneau 2010). Together with the bending moment (M) and shear force (V) acting on the beam, the forces applied to the beam is schematically shown in Fig. 2.

$$\omega_{ybi} = f_{yp} t_{wi} \left(\cos\alpha\right)^2 \tag{1}$$

$$\omega_{xbi} = \frac{1}{2} f_{yp} t_{wi} \sin 2\alpha \tag{2}$$

3. Boundary effects

It has been well-recognized that Euler-Bernoulli beam theory can be applied to design a typical structural H-shaped beam in engineering applications. The derivation is based upon the assumption that the cross section of the beam is always perpendicular to the bending line. The mathematical expression can be given by Eq. (3). In practical design, the contribution of the flanges to the shear force is generally neglected and the maximum shear stress in the beam can therefore be estimated by assuming that the shear force is totally and uniformly carried by the beam web, as shown in Eq. (4).

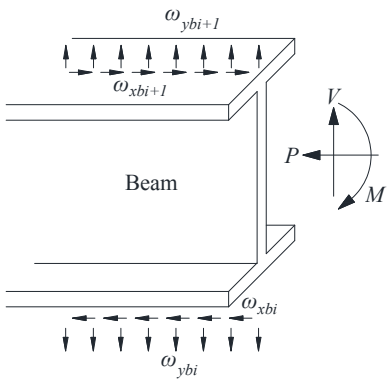

Fig. 2 Forces acting on the beam

$$\tau = \frac{VS}{I_b t_{bw}} \tag{3}$$

$$\tau = \frac{V}{h_w t_{bw}} \tag{4}$$

However, severe damages were observed in many moment resisting frame buildings during the Northridge and Kobe earthquakes. Causes of the observed damage had been the subject of considerable discussion and had been classified into three classes in general (Chen and Yamaguchi 1995): welding-related factors, design-related factors, and material-related factors. Among them the presence of triaxial tensile stress state and high strain rate was an essential factor that contributed to the brittle fracture at the beam-to-column connections. Furthermore, it was understood that the connection failures during the Northridge earthquake were to some extent, due to the three-dimensional restraint in the connection region. The restraint provided by the column flange does not allow the expected ductile yielding of the beam flanges (Miller 1998).

To clearly describe the unexpected failure in the beam-to-column connections, it should be noted firstly that the assumption that the shear force is transferred through the beam web to the column face only holds where the Euler-Bernoulli hypothesis is still valid. As a matter of fact, beam-to-column connection region is under boundary condition and the cross section of a beam will not remain plane under external forces, where Saint-Venant Principle follows:

"*If the forces acting on a small portion of the surface of an elastic body are replaced by another statically equivalent system of forces acting on the same portion of the surface, this redistribution of loading produces substantial changes in the stresses locally but has a negligible effect on the stresses at distances which are large in comparison with the linear dimensions of the surface on which the forces are changed.*"

In other words, the force transfer path and stress distribution mechanism at the beam-to-column connections at distances which are comparable to the cross-sectional dimension of the beam differ dramatically from the traditional knowledge and are much more complicated due to the complex geometrical configuration and strong restraint.

Considering two randomly-selected elements A and B in the beam as illustrated in Fig. 3, element A is located at a distance considerably far away from the column face, and element B is adjacent to the connection boundary region. The relations between the normal strains (ε_x, ε_y, ε_z) and normal stresses (σ_x, σ_y, σ_z) for these two elements can be determined according to Hooke's Law as

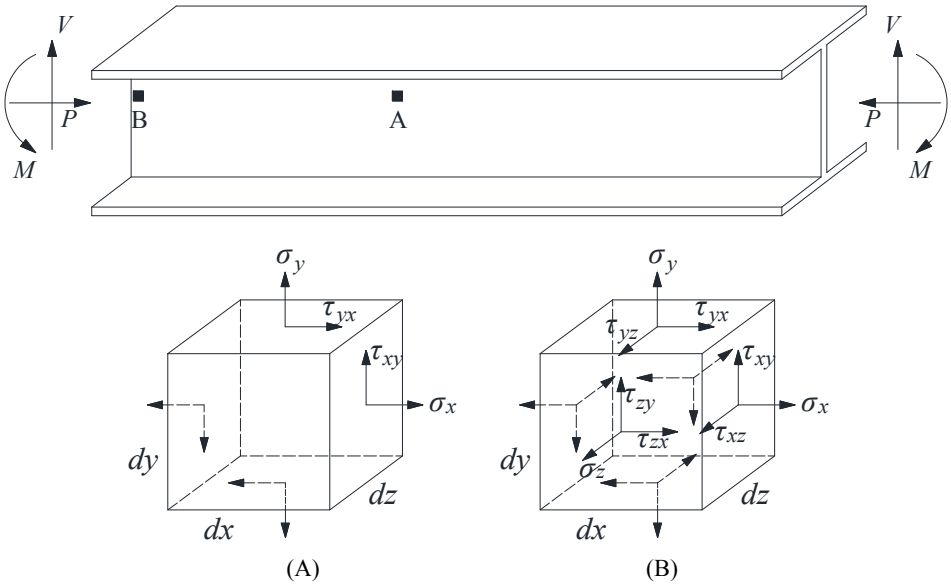

Fig. 3 stress conditions in the beam

$$\varepsilon_x = \frac{1}{E}\left[\sigma_x - \nu\left(\sigma_y + \sigma_z\right)\right] \tag{5a}$$

$$\varepsilon_y = \frac{1}{E}\left[\sigma_y - \nu\left(\sigma_z + \sigma_x\right)\right] \tag{5b}$$

$$\varepsilon_z = \frac{1}{E}\left[\sigma_z - \nu\left(\sigma_x + \sigma_y\right)\right] \tag{5c}$$

For element *A*, as the beam can deform freely in any directions and no force is applied in the *z*-direction, i.e., σ_z = 0, the plane stress condition is satisfied and Eqs. 5(a)-(c) can be reduced as

$$\varepsilon_x = \frac{1}{E}\left(\sigma_x - \nu\sigma_y\right) \tag{6a}$$

$$\varepsilon_y = \frac{1}{E}\left(\sigma_y - \nu\sigma_x\right) \tag{6b}$$

$$\varepsilon_z = -\frac{\nu}{E}\left(\sigma_x + \sigma_y\right) \tag{6c}$$

Note that the normal stress σ_x in the *x*-direction is resulted from bending moment *M* and axial force *P*, while the normal stress σ_y in the *y*-direction is caused by the vertical component of inclined tension field on the beam. Also note that axial force *P* generates negative normal stress in the cross-section of beam, while bending moment *M* generates positive and negative normal stresses in the upper half and lower half of beam depth, respectively, where negative stress denotes compression and positive stress denotes tension.

It can be found from Eq. (6b) that a positive value of σ_x (tension) leads to the reduction in ε_y while the negative σ_x (compression) results in greater ε_y. Therefore, the depth of beam in the upper region, which is under tension along the *x*-direction, tends to be shorter along the *y*-direction, while the depth of beam in the lower part, subjected to compression in the *x*-direction, tends to be longer along the *y*-direction. The deforming trend in the *z*-direction can be obtained from Eq. (6c) the width of the beam tends to be narrower in the upper part while tends to be wider in the lower part.

Things become more complicated when the stress condition of element *B* is explored. Element B is close to the beam-to-column boundary and the deformation of the beam is likely fix-restrained by the column face. Thus, the normal strains ε_x, ε_y, and ε_z in Eqs. 5(a)-(c) should be zero along the restraining line. Under this condition, additional normal stresses in the *y* and *z* directions, $\sigma_{y,a}$ and $\sigma_{z,a}$, respectively, should be generated to balance the normal strain induced by σ_x and σ_y. For the upper part of the beam, $\sigma_{y,a}$ should be positive to alleviate the "depressed" trend of beam depth, while $\sigma_{z,a}$ should be positive to prevent the beam from getting narrower. In contrast, $\sigma_{y,a}$ should be negative in the lower part of beam to alleviate the "extruded" trend, while $\sigma_{z,a}$ should be negative to restrain the beam from becoming wider. Therefore, due to the boundary constraint, additional shear strains are induced near the connection, which additionally causes additional shear stress. The shear stress is in the same direction of the applied shear force at the top and bottom parts of the beam while in the opposite direction of the applied shear force in the middle part of the beam to remain force equilibrium. In other words, the shear force moves towards the beam flanges at the connection.

4. Plastic flexural capacity of beam in SPSW

4.1 Reduced plastic flexural capacity in the flange

For the beam cross section adjacent to the column face, i.e., within the region of $0.5d_b$ (Arlekar and Murty 2004) away from the connection, the stress distribution is altered significantly due to the boundary effects (or Saint Venant

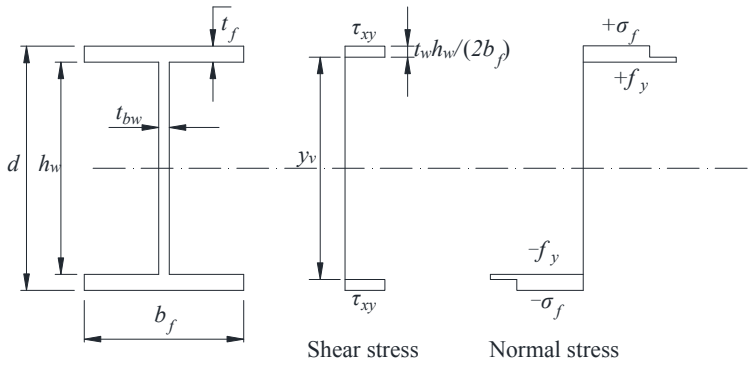

Fig. 4 Plastic flexural capacity of beam flange considering boundary effects

effects), and the division of the role between the flanges and the web, as predicted by classical Euler-Bernoulli theory, cannot be achieved. The flanges carry both bending moment and shear force, while the beam web carries bending moment and axial force and is devoid of shear stress near the neutral axis. Fig. 4 shows the plastic flexural capacity of the beam flange considering boundary effects. Assuming the magnitude of shear force in the beam flange is equal to that previously carried by beam web, the devoid region of shear stress in the beam, y_v, is given by Eq. (7). It should be noted that this assumption satisfy the condition that the shear force is carried by the beam flanges instead of beam web at the connection as described in detail in Section 3.

$$y_v = d - \frac{t_{bw} h_w}{b_f} \tag{7}$$

According to von Mises criterion, both normal stress and shear stress participate in yielding the section. Consequently, the maximum x-direction normal stress (σ_f) that can be applied on the beam flanges is given as

$$\sigma_f = \sqrt{f_y^2 - 3\tau_{xy}^2} \tag{8}$$

τ_{xy} can be calculated from Eq. (4). Therefore, the yield strength of some region of flanges which carry both shear stress and normal stress is reduced to σ_f due to the shear concentration on the flanges resulted from the boundary effect.

The contributions of the flanges ($M_{flange}^{B-M,V}$) to plastic flexural capacity can be calculated based on the flexural stress diagrams as

$$M_{flange}^{B-M,V} = \frac{h_w t_{bw}}{2}\left(d - \frac{t_{bw} h_w}{2b_f}\right)\sigma_f + \left(t_f b_f - \frac{t_{bw} h_w}{2}\right)\left(d - t_f - \frac{t_{bw} h_w}{2b_f}\right) f_y \tag{9}$$

Although it is possible to calculate the plastic flexural capacity of beam flange based on Eq. (9), it is still somewhat complicated for engineer use and thus, the design procedure is better to be further simplified. Therefore, in this research, proper assumptions and simplifications were made to reduce the formula's complexity to a reasonable level. As a matter of fact, Eq. (7) normally results in $y_v \geq h_w$ for practical beam size that is used in design, which means the entire HBE web is inactive in carrying the shear force. Consequently, it can be assumed that the flanges are subjected to combined flexure and shear, while the web is under flexure and tension as shown in Fig. 5. It should be noted that the assumption offers slightly lower value of plastic flexural capacity of beam flanges and is on the conservative side. Therefore, the shear stress is assumed to be carried uniformly by the beam flange and is given as

$$\tau_{xy} = \frac{V}{2b_f t_f} \tag{10}$$

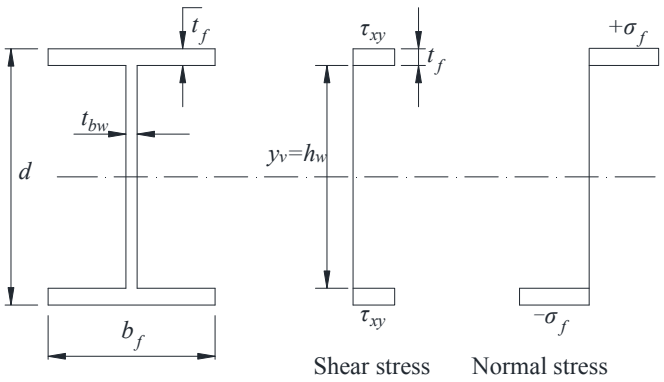

Fig. 5 Simplified flexural stress diagrams

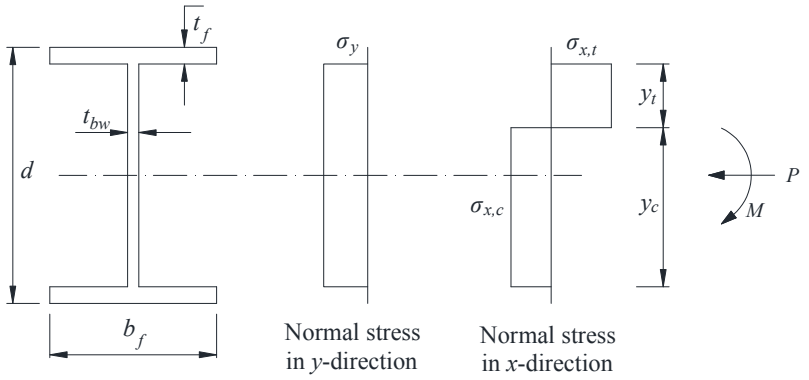

Fig. 6 Stress condition in the beam web

In this case, Eq. (9) is reduced to

$$M_{flange}^{B-M,V} = t_f b_f \left(d - t_f\right)\sigma_f \tag{11}$$

4.2 Reduced plastic flexural capacity in the web

Due to the presence of vertical component of tension field on the beam, the plastic flexural capacity of the beam web should be reduced according to the research by Qu and Bruneau (2011). This section presents the design procedures for prediction of reduced plastic flexural capacity in the web according to the plane stress state, which resembles the method used by pervious researchers such as Qu and Bruneau (2011). However, in this research, the shear stress is absent in the web due to the boundary effect. The normal stress σ_y in the y-direction in the web under the condition of equal top and bottom tension fields can be calculated as (Qu and Bruneau 2011)

$$\sigma_y = \frac{\omega_{ybi}}{t_{bw}} \tag{12}$$

Considering an element randomly selected from the beam web, it is under plane stress state. Since no shear force exists in the web, the normal stresses σ_x and σ_y in the x and y directions, respectively, become the principal stresses.

For steel under multi-axial plane-stress conditions and owning uniaxial elasto-perfectly plastic behavior, von Mises yield criterion can be used and expressed as

$$f_y = \sqrt{\sigma_x^2 - \sigma_x\sigma_y + \sigma_y^2} \tag{13}$$

Eq. (13) can be regarded as a quadratic function in terms of σ_x and gives

$$\sigma_{x,t} = \frac{1}{2}\sigma_y + \frac{1}{2}\sqrt{4f_y^2 - 3\sigma_y^2} \tag{14}$$

$$\sigma_{x,c} = \frac{1}{2}\sigma_y - \frac{1}{2}\sqrt{4f_y^2 - 3\sigma_y^2} \tag{15}$$

Fig. 6 shows the plastic flexural capacity of beam web. The reader is referred to Qu and Bruneau (2011) for background and for the derivation of compression (y_c) and tension (y_t) portion of the web, which is given by Eqs. (16) and (17), respectively

$$y_c = \frac{\left(\frac{\sigma_{x,t}}{f_y}\right) + \beta_w}{\left(\frac{\sigma_{x,t}}{f_y}\right) - \left(\frac{\sigma_{x,c}}{f_y}\right)} \cdot h_w \tag{16}$$

$$y_t = h_w - y_c \tag{17}$$

$$\beta_w = -\frac{P}{f_y h_w t_{bw}} \tag{18}$$

The contribution of the web to the plastic flexural capacity, $M_{web}^{M,P}$, can then be determined according to the stress diagram in Fig. 6 as

$$M_{web}^{M,P} = \sigma_{x,t} t_{bw} y_t \left(\frac{h_w}{2} - \frac{y_t}{2}\right) - \sigma_{x,c} t_{bw} y_c \left(\frac{h_w}{2} - \frac{y_c}{2}\right) \tag{19}$$

4.3 Reduced plastic flexural capacity of beam

Taking into account the boundary effects as detailed in Section 4.1 and using the reduced axial yield strength obtained from the von Mises yield criterion accounting for the vertical stress as presented in Section 4.2, the reduced plastic flexural capacity of the beam ($M_b^{M,V,P}$) subjected to combined bending moment, shear force, and axial compression can be obtained based on the superposition of the reduced plastic flexural capacity of the flanges ($M_{flange}^{B-M,V}$) and the contribution of the web ($M_{web}^{M,P}$), given as

$$M_b^{M,V,P} = M_{flange}^{B-M,V} + M_{web}^{M,P} \tag{20}$$

5. Validation for the proposed equation

5.1 Comparison with Qu (2008)

In order to validate the accuracy of the proposed formula, the theoretical results from the formula proposed above are firstly compared to the data in Qu's study (2008).

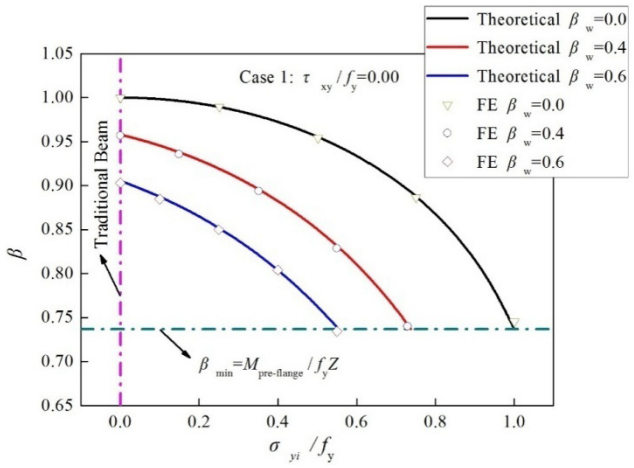

(a) For $\tau_{xy}/f_y = 0.00$

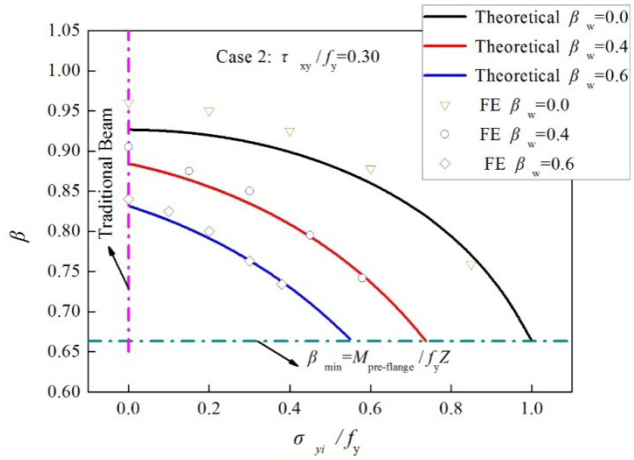

(b) For $\tau_{xy}/f_y = 0.30$

Fig. 7 Comparison of theoretical results and Qu (2008)

Qu (2008) developed a two-phase experimental program to test a full-scale two story SPSW specimen, as part of the MCEER/NCREE collaborative research program. However, the focus of the experiments is to address the replaceability of infill panels following an earthquake and thus, the beams did not fully exhibit their plastic capacities. Some extra numerical analyses have been conducted by Qu (2008) and the reasonability of the FE models has been well calibrated with a number of experiments. In this study, these FE models were selected to comprehensively calibrate the proposed formula. The reader is referred to Qu (2008) for detailed information of the numerical models.

In the study of Qu (2008), a cross section plastic flexural capacity reduction factor, β, is defined to measure the loss in plastic flexural capacity. The value of β can be determined as

$$\beta = \frac{M_b^{M,V,P}}{f_y Z} \tag{21}$$

The comparison is shown in Fig. 7. It can be found that, in general, the cross-section plastic moment reduction factors predicted by the formula proposed in the present study agrees well the FE analysis. The ratio of the predicted values to the numerical ones based on the proposed model range from 0.963 to 1.016 with a mean of 0.993 and a standard deviation of 0.014. These values closely corresponded. Meanwhile, it is obvious that an increase of the τ_{xy} values leads to a decrease in the beam cross section plastic moment. Fig. 7 also shows that for beams with $\tau_{xy}/f_y = 0$, the mean value of the ratio of the theoretical results to the FE ones equals to 1.001 while the corresponding standard deviation is 0.004, which means the proposed calculation method can well predict the flexure behavior of beams where the shear force is absent. On the other hand, for beams with $\tau_{xy}/f_y = 0.3$, the predicted values slightly underestimate the real plastic moment. This is because the assumption is made on the conservative side in Section 4.1 that the entire cross-sectional areas of the flanges is under combined flexure and shear, in order to simplify Eq. (9) to Eq. (11) for easy hand calculation. This would slightly underestimate the flexural capacity of the flanges. It also should be noted that the boundary column was not included in Qu's model. The lack of restraint of column face to the beam does not exactly reflect the boundary effect presented in this paper. Furthermore, for a given value of τ_{xy} and β_w, when the tension field induced by infill panel increases from zero to around 0.3, the cross section plastic moment reduction factor gradually reduces from unity to a certain value. Beyond that, the cross section plastic moment reduction factor decreases quickly to a minimum. In addition, both the increase in the axial force and shear lead to a decrease of the developed plastic moment in the beam.

5.2 Comparison with Berman and Bruneau (2008)

Berman and Bruneau (2008) used the MCEER demonstration hospital as the prototype structures for design of SPSW. The Specimen SPSW-C with equal thickness of web plates at each story was selected in this paper for discussion. The general information about the specimen is summarized herein. The reader is referred to Berman and Bruneau for detailed model information. Specimen SPSW-C had the boundary columns with cross sections of W40×593, anchor beams with cross sections of W40×331, intermediate beams with cross sections of W21×73, and web plate thickness of 4.7625 mm. ASTM A36 was used for web plates and ASTM A992 was for the beams. The applied shear force and axial compression on the beam are listed in Table 1. It should be noted that in Specimen SPSW-C, the axial compression P in the beams at 2nd and 3rd stories results in the value of β_w greater than 1.0, which means that both the entire web cross section and some region of flanges are used to carry the axial compression. Therefore, only part of flanges are active in resisting the bending moment. The comparison is given in

Table 1 Comparison of theoretical results and Berman and Bruneau (2008)

Specimen	Story	P (kips)	V (kips)	M (kip-in.)	M_p (kip-in.)	M_p / M
SPSW-C	2	–622	28	4095	4555	1.11
	3	–537	33	4864	5399	1.11

Table 1. It can be observed that the ratio of the predicted plastic flexural capacity M_p to the design bending moment M is 1.11, which means that the boundary beam is able to sustain the applied loads on the structures and is consistent with the results by Berman and Bruneau (2008).

6. Conclusions

A methodology for the manual calculation procedure to predict the plastic flexural capacity of beams in SPSW is mainly discussed in this paper. The main contribution of this paper is to consider the boundary effect to actualize the force transfer mechanism in the beams. The reduction of strength in beam web was introduced and modified based on the study by Qu and Bruneau (2011), while the shear stress is absent in the web in this research due to the boundary effect. The following conclusions are based on the results and observations presented herein.

(1) The proposed methodology for the beam plastic flexural capacity is based on the modified classical beam theory and plastic analysis, which assembles the methods by Qu and Bruneau (2011). The plastic flexural capacity of the beams is given by the superposition of the contribution from the web and the flanges.
(2) The influence of boundary effect is comprehensively discussed. According to the Saint Venant effects, the shear stresses would be transferred to the beam flanges from the web near the column face, leaving most of the beam web devoid of shear.
(3) Comparisons made with previous research show that the proposed equations provide remarkably accurate predictions of the beam behavior that are suitable for use.

It should be mentioned that the research in this paper is based on the assumption that both web plate above and below the beam are with the same thickness and both yielded. In real practical cases it may happen that the plates with different thicknesses are used. This will cause the developed tension fields are different on two beam sides. The authors are currently working on establishing design method for flexural behavior of SPSW with unequal tension fields that will be presented in future publications.

Acknowledgments

This work is sponsored by A Project Funded by the Priority Academic Program Development of Jiangsu Higher Education Institutions (PAPD) and Prospective Joint Research Project of Jiangsu Province, China (Grant No. BY2016076-06). The authors also appreciate the original idea on design of beam in SPSWs by Professor Michel Bruneau at University at Buffalo, Professor Jeffrey W. Berman at University of Washington, and Professor Bing Qu at California Polytechnic State University, which provides solid basis for the development of this paper.

References

ANSI/AISC 341-10 (2010), Seismic Provisions for Structural Steel Buildings, American Institute of Steel Construction, Chicago, IL, USA.
Arlekar, J.N. and Murty, C.V.R. (2004), "Improved truss model for design of welded steel moment-resisting frame connections", *J. Struct. Eng.*, **130**(3), 498-510.
Bahrebar, M., Kabir, M.Z., Hajsadeghi, M., Zirakian, T. and Lim, J.B.P. (2016), "Structural performance of steel plate. shear walls with trapezoidal corrugations and centrally-placed square perforations", *Int. J. Steel Struct.*, **16**(3), 845-855.
Berman, J. and Bruneau, M. (2003), "Plastic analysis and design of steel plate shear walls", *J. Struct. Eng.*, **129**(11), 1448-1456.
Berman, J.W. and Bruneau, M. (2008), "Capacity design of vertical boundary elements in steel plate shear walls", *Eng. J. AISC*, **45**(1), 57-71.
CAN/CSA S16-14 (2014), Design of Steel Structures, Canadian Standards Association, Willowdale, ON, Canada.
Chatterjee, A.K., Bhowmick, A. and Bagchi, A. (2015), "Development of a simplified equivalent braced frame model for steel plate shear wall systems", *Steel Comp. Struct., Int. J.*, **18**(3), 711-737.
Chen, W.F. and Yamaguchi, E. (1995), Connection failure of steel moment-frame buildings during the Northridge earthquake, Report CE-STR-95-12, School of Civil Engineering, Purdue University, USA.
Clayton, P.M., Berman, J.W. and Lowes, L.N. (2013), "Subassembly testing and modeling of self-centering steel plate shear walls", *Eng. Struct.*, **56**, 1848-1857.
Dhar, M.M. and Bhowmick, A.K. (2016), "Seismic response estimation of steel plate shear walls using nonlinear static methods", *Steel Comp. Struct., Int. J.*, **20**(4), 777-799.
Guo, L., Rong, Q., Ma, X. and Zhang, S. (2011), "Behavior of steel plate shear wall connected to frame beams only", *Int. J. Steel Struct.*, **11**(4), 467-479.
Guo, Z. and Yuan, Y. (2015), "Experimental study of steel plate composite shear wall units under cyclic load", *Int. J. Steel Struct.*, **15**(3), 515-525.
He, L., Kurata, M. and Nakashima, M. (2015), "Condition assessment of steel shear walls with tapered links under various loadings", *Earthq. Struct., Int. J.*, **9**(4), 767-788.
JGJ/T380-2015 (2015), Technical specification for steel plate shear walls, Ministry of Housing and Urban-Rural Development, Beijing, China.
Lee, C.H. (2006), "Review of force transfer mechanism of welded steel moment connections", *J. Constr. Steel Res.*, **62**(7), 695-705.
Lee, C.H. and Yoon, T.H. (1999), "Analytical re-examination of shear transfer in welded steel moment connection", *Proceedings of the 1st Japan-Korea Joint Seminar on Earthquake Engineering for Building Structures*.
Lubell, A.S., Prion, H.G.L., Ventura, C.E. and Rezai, M. (2010), "Unstiffened steel plate shear wall performance under cyclic loading", *J. Struct. Eng.*, **126**(4), 453-460.
Miller, D.K. (1998), "Lessons learned from the Northridge earthquake", *Eng. Struct.*, **20**(4-6), 249-260.
Moghimi, H. and Driver, R.G. (2014), "Beam design force demands in steel plate shear walls with simple boundary frame connections", *J. Struct. Eng.*, **140**(7), 04014046.
Park, H.G., Kwack, J.H., Jeon, S.W., Kim, W.K. and Choi, I.R. (2007), "Frame steel plate wall behavior under cyclic lateral loading", *J. Struct. Eng.*, **133**(3), 378-388.
Qu, B. (2008), "Seismic behavior and design of boundary frame members of steel plate shear walls", Ph.D. Thesis; The State University of New York at Buffalo, Buffalo, NY, USA.
Qu, B. and Bruneau, M. (2010), "Capacity design of intermediate

horizontal boundary elements of steel plate shear walls", *J. Struct. Eng.*, **136**(6), 665-675.
Qu, B. and Bruneau, M. (2011), "Plastic moment of intermediate horizontal boundary elements of steel plate shear walls", *Eng. J. AISC*, **48**(1), 49-64.
Rahmzadeh, A., Ahmad; Ghassemieh, M., Park, Y. and Abolmaali, A. (2016), "Effect of stiffeners on steel plate shear wall systems", *Steel Comp. Struct., Int. J.*, **20**(3), 545-569.
Sabouri-Ghomi, S. and Mamazizi, S. (2015), "Experimental investigation on stiffened steel plate shear walls with two rectangular openings", *Thin-Wall. Struct.*, **86**, 56-66.
Sahoo, D.R., Sidhu, B.S. and Kumar, A. (2015), "Behavior of unstiffened steel plate shear wall with simple beam-to-column connections and flexible boundary elements", *Int. J. Steel Struct.*, **15**(1), 75-87.
Thorburn, L.J., Kulak, G.L. and Montgomery, C.J. (1983), Analysis of steel plate shear walls, Structural Engineering Report No. 107; Department of Civil Engineering, University of Alberta, Edmonton, Alberta, Canada.
Timler, P.A. and Kulak, G.L. (1983), Experimental study of steel plate shear walls, Structural Engineering Report No. 114; Department of Civil Engineering, University of Alberta, Edmonton, AB, Canada.
Vatansever, C. and Berman, J.W. (2015), "Analytical investigation of thin steel plate shear walls with screwed infill plate", *Steel Compos. Struct., Int. J.*, **19**(5), 1145-1165.
Zirakian, T. and Zhang, J. (2015), "Seismic design and behavior of low yield point steel plate shear walls", *Int. J. Steel Struct.*, **13**(1), 163-174.

CC

Notation

b_f	width of beam flange
d	beam depth
E	elastic modulus of steel
f_y	yield strength of steel
f_{yp}	yield strength of web plates
h_w	depth of beam web
M	bending moment acting on the beam
$M_{flange}^{B-M,V}$	contribution of the flanges to plastic flexural capacity
M_{web}	contribution of the web to the plastic flexural capacity
P	axial compressive force acting on the beam
S	statical moment of area
t_{bw}	thickness of the beam web
t_f	thickness of beam flange
t_{wt}	thickness of web plates at ith story
V	shear force acting on the beam
y_c, y_t	compression and tension portion of the web, respectively
y_v	devoid region of shear stress in the beam
Z	plastic section modulus of the beam
α	angle of the tension field
ω_{xbi}, ω_{ybi}	horizontal and vertical components of web plates tension fields on beams, respectively
σ_f	maximum x-direction normal stress in the beam flange
σ_x, σ_y	normal stresses in the x and y directions, respectively
$\sigma_{x,t}$, $\sigma_{x,c}$	tension and compression normal stress in the x-directions, respectively
τ	shear stress in the beam
τ_{xy}	shear stress in the beam flange
v	Poisson's ratio
ε_x, ε_y, ε_z	normal strains in the x, y, and z directions, respectively
σ_x, σ_y, σ_z	normal stresses in the x, y, and z directions, respectively
β	cross section plastic flexural capacity reduction factor
β_w	ratio of the applied axial compression force to the nominal axial strength of the beam web